REPORT DOCUMENTATION PAGE

Form Approved OMB NO. 0704-0188

1. REPORT DATE (DD-MM-YYYY)	2. REPORT TYPE	3. DATES COVERED (From - To)
10-05-2010	Final Report	1-Sep-2003 - 31-Mar-2007

4. TITLE AND SUBTITLE

Ultrafast Mid-Infrared Dynamics in Quantum Cascade Lasers

5a. CONTRACT NUMBER

DAAD19-03-1-0300

5b. GRANT NUMBER

5c. PROGRAM ELEMENT NUMBER

611102

6. AUTHORS

T. B. Norris

5d. PROJECT NUMBER

5e. TASK NUMBER

5f. WORK UNIT NUMBER

7. PERFORMING ORGANIZATION NAMES AND ADDRESSES

University of Michigan - Ann Arbor
Room 1058 Wolverine Tower
3003 South State Street
Ann Arbor, MI   48109 -1274

8. PERFORMING ORGANIZATION REPORT NUMBER

9. SPONSORING/MONITORING AGENCY NAME(S) AND ADDRESS(ES)

U.S. Army Research Office
P.O. Box 12211
Research Triangle Park, NC 27709-2211

10. SPONSOR/MONITOR'S ACRONYM(S)

ARO

11. SPONSOR/MONITOR'S REPORT NUMBER(S)

45151-PH.1

12. DISTRIBUTION AVAILIBILITY STATEMENT

Approved for Public Release; Distribution Unlimited

13. SUPPLEMENTARY NOTES

The views, opinions and/or findings contained in this report are those of the author(s) and should not contrued as an official Department of the Army position, policy or decision, unless so designated by other documentation.

14. ABSTRACT

This report summarizes the entire research period. In this program, we performed experiments using a femtosecond mid-infrared pump-probe system implemented for QCL samples operating at 4.6 and 5.3 μm. We employed femtosecond time-resolved pump-probe measurements to probe the nature of the transport through the laser structure via the dynamics of the gain. The gain recovery was determined by the time-dependent transport of electrons through the cascade heterostructure; as the laser approaches and exceeds threshold, the gain recovery

15. SUBJECT TERMS

ultrafast spectroscopy, quantum dots, quantum cascade lasers

16. SECURITY CLASSIFICATION OF:			17. LIMITATION OF ABSTRACT	15. NUMBER OF PAGES	19a. NAME OF RESPONSIBLE PERSON
a. REPORT	b. ABSTRACT	c. THIS PAGE	UU		Theodore Norris
UU	UU	UU			19b. TELEPHONE NUMBER
					734-764-9269

Report Title

Ultrafast Mid-Infrared Dynamics in Quantum Cascade Lasers

ABSTRACT

This report summarizes the entire research period. In this program, we performed experiments using a femtosecond mid-infrared pump-probe system implemented for QCL samples operating at 4.6 and 5.3 μm. We employed femtosecond time-resolved pump-probe measurements to probe the nature of the transport through the laser structure via the dynamics of the gain. The gain recovery was determined by the time-dependent transport of electrons through the cascade heterostructure; as the laser approaches and exceeds threshold, the gain recovery shows a dramatic reduction due to the onset of quantum stimulated emission. Since the electron transport through each state in the cascade is determined by the state lifetime, the transport in a cascade laser is driven by the photon density in the cavity. The gain recovery is qualitatively different from that in conventional atomic, molecular and interband semiconductor lasers due to the superlattice transport in the cascade. We also studied the effects of pulse propagation in the laser, including group velocity dispersion and coherent pulse reshaping due to ultrafast Rabi flopping of the gain medium.

List of papers submitted or published that acknowledge ARO support during this reporting period. List the papers, including journal references, in the following categories:

(a) Papers published in peer-reviewed journals (N/A for none)

Hyunyong Choi, Laurent Diehl, Zong-kwei Wu, Marcella Giovannini, Jerome Faist, Federico Capasso, and Theodore B. Norris "Time-Resolved Investigations of Electronic Transport Dynamics in Quantum Cascade Lasers Based on Diagonal Lasing Transition," IEEE. J. Quant. Electron. 45, 307 (2009).

Hyunyong Choi, Laurent Diehl, Marcella Giovannini, Jerome Faist, Federico Capasso, and Theodore B. Norris, "Femtosecond pump-probe studies of carrier transport and gain dynamics in quantum cascade lasers," phys. stat. sol. (c) 5, 225 (2008).

Hyunyong Choi, Laurent Diehl, Federico Capasso, David Bour, Scott Corzine, Jintian Zhu, Gloria Höfler, and Theodore B. Norris, "Time-domain upconversion measurements of group-velocity dispersion in quantum cascade lasers," Opt. Express 15, 15898 (2007).

H. Choi, L. Diehl, Z-K. Wu, M. Giovannini, J. Faist, F. Capasso, T.B. Norris , "Gain Recovery Dynamics and Photon-Driven Transport in Quantum Cascade Lasers," Phys. Rev. Lett. 100, 167401 (2008).

H. Choi, T.B. Norris, T. Gresch, M. Giovanni, J. Faist, L. Diehl, and F. Capasso, "Femtosecond Dynamics of Resonant Tunneling and Superlattice Relaxation in Quantum Cascade Lasers," Appl. Phys. Lett. 92, 122114 (2008).

Number of Papers published in peer-reviewed journals:　　　　5.00

(b) Papers published in non-peer-reviewed journals or in conference proceedings (N/A for none)

Number of Papers published in non peer-reviewed journals:　　　　0.00

(c) Presentations

H. Choi, V.-M. Gkortsas, F. X. Kärtner, L. Diehl, C.-Y. Wang, F. Capasso, D. Bour, S. Corzine, J. Zhu, G. Hofler, and T. B. Norris, "Femtosecond resonant pulse propagation in quantum cascade lasers: evidence of coherent effects," CLEO/QELS 2008, San Jose, CA, May 2008.

H. Choi, T. B. Norris, L. Diehl, F. Capasso, D. Bour, S. Corzine, J. Zhu, and G. Hofler, "Time-domain measurements of group-velocity dispersion in quantum cascade lasers," CLEO/QELS 2008, San Jose, CA, May 2008.

T.B. Norris, "Dynamics of Photon-Assisted Transport in Quantum Cascade Lasers," Fundamental Optical Processes in Semiconductors, Big Sky 2007.

Hyunyong Choi, Laurent Diehl, Marcella Giovannini, Jérôme Fais, and Federico Capasso, Theodore B. Norris, "Dynamics of Photon-Driven Electron Transport in InGaAs/InAlAs Quantum Cascade Lasers", 9th International Conference on Intersubband Transitions in Quantum Wells, Ambleside, United Kingdom, Sep 2007.

Hyunyong Choi, Laurent Diehl, Marcella Giovannini, Jérôme Fais, and Federico Capasso, Theodore B. Norris, "Observation of Photon-Driven Electronic Transport in Quantum Cascade Lasers", CLEO-PR, Seoul, Korea, Aug 2007.

Hyunyong Choi, Laurent Diehl, Tobias Gresch, Marcella Giovannini, Jérôme Fais, and Federico Capasso, Theodore B. Norris, "Femtosecond Pump-Probe Studies of Carrier Transport and Gain Dynamics in Quantum Cascade Lasers", 15th International Conference on Nonequilibrium Carrier Dynamics in Semiconductors (HCIS-15), Tokyo, Japan, Jul 2007.

Hyunyong Choi, Zong-Kwei Wu, Theodore B. Norris, Tobias Gresch, Marcella Giovannini, Jérôme Fais, Laurent Diehl and Federico Capasso, "Time-Resolved Studies of Gain Dynamics in Quantum Cascade Laser," American Institute of Physics Proceedings on the 28th International Conference on the Physics of Semiconductors, vol 893, 2007.

Hyunyong Choi, Laurent Diehl, Marcella Giovannini, Jérôme Fais, and Federico Capasso, Theodore B. Norris, ``Photon-Driven Transport in Quantum Cascade Lasers'', paper CThO3 presented at CLEO/QELS, Baltimore, MD, May 2007.

Hyunyong Choi, Zong-Kwei Wu, Theodore B. Norris, Tobias Gresch, Marcella Giovannini, Jérôme Fais, Laurent Diehl and Federico Capasso, "Time-Resolved Studies of Gain Dynamics in Quantum Cascade Laser," ICPS-28, Vienna, Austria, Jun 2006.

Hyunyong Choi, Zong-Kwei Wu, Theodore B. Norris, Tobias Gresch, Marcella Giovannini, Jérôme Fais, Laurent Diehl and Federico Capasso, "Ultrafast Gain Dynamics in a Quantum Cascade Laser," paper JTuD98 presented at CLEO/QELS, Long Beach, CA, 2006.

Number of Presentations: 10.00

Non Peer-Reviewed Conference Proceeding publications (other than abstracts):

Number of Non Peer-Reviewed Conference Proceeding publications (other than abstracts):   0

Peer-Reviewed Conference Proceeding publications (other than abstracts):

Number of Peer-Reviewed Conference Proceeding publications (other than abstracts):   0

(d) Manuscripts

Number of Manuscripts: 0.00

Patents Submitted

Patents Awarded

Graduate Students

NAME	PERCENT_SUPPORTED
Hyungyong Choi	0.50
FTE Equivalent:	**0.50**
Total Number:	**1**

Names of Post Doctorates

NAME	PERCENT_SUPPORTED
FTE Equivalent:	
Total Number:	

Names of Faculty Supported

NAME	PERCENT_SUPPORTED	National Academy Member
Theodore B. Norris	0.08	Yes
Hyunyong Choi	0.50	No
FTE Equivalent:	**0.58**	
Total Number:	**2**	

Names of Under Graduate students supported

NAME	PERCENT_SUPPORTED
FTE Equivalent:	
Total Number:	

Student Metrics
This section only applies to graduating undergraduates supported by this agreement in this reporting period

The number of undergraduates funded by this agreement who graduated during this period: 0.00

The number of undergraduates funded by this agreement who graduated during this period with a degree in science, mathematics, engineering, or technology fields:...... 0.00

The number of undergraduates funded by your agreement who graduated during this period and will continue to pursue a graduate or Ph.D. degree in science, mathematics, engineering, or technology fields:...... 0.00

Number of graduating undergraduates who achieved a 3.5 GPA to 4.0 (4.0 max scale):...... 0.00

Number of graduating undergraduates funded by a DoD funded Center of Excellence grant for Education, Research and Engineering:...... 0.00

The number of undergraduates funded by your agreement who graduated during this period and intend to work for the Department of Defense 0.00

The number of undergraduates funded by your agreement who graduated during this period and will receive scholarships or fellowships for further studies in science, mathematics, engineering or technology fields:...... 0.00

Names of Personnel receiving masters degrees

NAME
Total Number:

Names of personnel receiving PHDs

<u>NAME</u>
Hyunyong Choi

Total Number: 1

Names of other research staff

<u>NAME</u>   <u>PERCENT_SUPPORTED</u>

 FTE Equivalent:
 Total Number:

Sub Contractors (DD882)

Inventions (DD882)

Ultrafast Mid-Infrared Dynamics in Quantum Cascade Lasers

Final Report

Principal Investigator:

Prof. Theodore B. Norris

Center for Ultrafast Optical Science

EECS Department, University of Michigan

2200 Bonisteel Blvd, Ann Arbor, MI 48109-2099

(734) 764-9269

Abstract

  This report summarizes the entire research period. In this program, we performed experiments using a femtosecond mid-infrared pump-probe system implemented for QCL samples operating at 4.6 and 5.3 µm. We employed femtosecond time-resolved pump-probe measurements to probe the nature of the transport through the laser structure via the dynamics of the gain. The gain recovery was determined by the time-dependent transport of electrons through the cascade heterostructure; as the laser approaches and exceeds threshold, the gain recovery shows a dramatic reduction due to the onset of quantum stimulated emission. Since the electron transport through each state in the cascade is determined by the state lifetime, the transport in a cascade laser is driven by the photon density in the cavity. The gain recovery is qualitatively different from that in conventional atomic, molecular and interband semiconductor lasers due to the superlattice transport in the cascade. We also studied the effects of pulse propagation in the laser, including group velocity dispersion and coherent pulse reshaping due to ultrafast Rabi flopping of the gain medium.

I. Research Summary

(1) List of Manuscripts

(a) submitted

Hyunyong Choi, Vasileios-Marios Gkortsas, Laurent Diehl, David Bour, Scott Corzine, Jintian Zhu, Gloria Höfler, Federico Capasso, Franz X. Kärtner, and Theodore B. Norris, "Ultrafast observation of Rabi flopping in a laser," submitted to Nature Physics.

(b) published

Hyunyong Choi, Laurent Diehl, Zong-kwei Wu, Marcella Giovannini, Jerome Faist, Federico Capasso, and Theodore B. Norris "Time-Resolved Investigations of Electronic Transport Dynamics in Quantum Cascade Lasers Based on Diagonal Lasing Transition," IEEE. J. Quant. Electron. 45, 307 (2009).

Hyunyong Choi, Laurent Diehl, Marcella Giovannini, Jerome Faist, Federico Capasso, and Theodore B. Norris, "Femtosecond pump-probe studies of carrier transport and gain dynamics in quantum cascade lasers," phys. stat. sol. (c) 5, 225 (2008).

Hyunyong Choi, Laurent Diehl, Federico Capasso, David Bour, Scott Corzine, Jintian Zhu, Gloria H¨ofler, and Theodore B. Norris, "Time-domain upconversion measurements of group-velocity dispersion in quantum cascade lasers," Opt. Express 15, 15898 (2007).

H. Choi, L. Diehl, Z-K. Wu, M. Giovannini, J. Faist, F. Capasso, T.B. Norris , "Gain Recovery Dynamics and Photon-Driven Transport in Quantum Cascade Lasers," Phys. Rev. Lett. 100, 167401 (2008).

H. Choi, T.B. Norris, T. Gresch, M. Giovanni, J. Faist, L. Diehl, and F. Capasso, "Femtosecond Dynamics of Resonant Tunneling and Superlattice Relaxation in Quantum Cascade Lasers," Appl. Phys. Lett. 92, 122114 (2008).

H. Choi, V.-M. Gkortsas, F. X. Kärtner, L. Diehl, C.-Y. Wang, F. Capasso, D. Bour, S. Corzine, J. Zhu, G. Hofler, and T. B. Norris, "Femtosecond resonant pulse propagation in quantum cascade lasers: evidence of coherent effects," CLEO/QELS 2008, San Jose, CA, May 2008.

H. Choi, T. B. Norris, L. Diehl, F. Capasso, D. Bour, S. Corzine, J. Zhu, and G. Hofler, "Time-domain measurements of group-velocity dispersion in quantum cascade lasers," CLEO/QELS 2008, San Jose, CA, May 2008.

T.B. Norris, "Dynamics of Photon-Assisted Transport in Quantum Cascade Lasers," Fundamental Optical Processes in Semiconductors, Big Sky 2007.

Hyunyong Choi, Laurent Diehl, Marcella Giovannini, Jérôme Fais, and Federico Capasso, Theodore B. Norris, "Dynamics of Photon-Driven Electron Transport in InGaAs/InAlAs

Quantum Cascade Lasers", 9th International Conference on Intersubband Transitions in Quantum Wells, Ambleside, United Kingdom, Sep 2007.

Hyunyong Choi, Laurent Diehl, Marcella Giovannini, Jérôme Fais, and Federico Capasso, Theodore B. Norris, "Observation of Photon-Driven Electronic Transport in Quantum Cascade Lasers", CLEO-PR, Seoul, Korea, Aug 2007.

Hyunyong Choi, Laurent Diehl, Tobias Gresch, Marcella Giovannini, Jérôme Fais, and Federico Capasso, Theodore B. Norris, "Femtosecond Pump-Probe Studies of Carrier Transport and Gain Dynamics in Quantum Cascade Lasers", 15th International Conference on Nonequilibrium Carrier Dynamics in Semiconductors (HCIS-15), Tokyo, Japan, Jul 2007.

Hyunyong Choi, Zong-Kwei Wu, Theodore B. Norris, Tobias Gresch, Marcella Giovannini, Jérôme Fais, Laurent Diehl and Federico Capasso, "Time-Resolved Studies of Gain Dynamics in Quantum Cascade Laser," American Institute of Physics Proceedings on the 28th International Conference on the Physics of Semiconductors, vol 893, 2007.

Hyunyong Choi, Laurent Diehl, Marcella Giovannini, Jérôme Fais, and Federico Capasso, Theodore B. Norris, ``Photon-Driven Transport in Quantum Cascade Lasers'', paper CThO3 presented at CLEO/QELS, Baltimore, MD, May 2007.

Hyunyong Choi, Zong-Kwei Wu, Theodore B. Norris, Tobias Gresch, Marcella Giovannini, Jérôme Fais, Laurent Diehl and Federico Capasso, "Time-Resolved Studies of Gain Dynamics in Quantum Cascade Laser," ICPS-28, Vienna, Austria, Jun 2006.

Hyunyong Choi, Zong-Kwei Wu, Theodore B. Norris, Tobias Gresch, Marcella Giovannini, Jérôme Fais, Laurent Diehl and Federico Capasso, "Ultrafast Gain Dynamics

in a Quantum Cascade Laser," paper JTuD98 presented at CLEO/QELS, Long Beach, CA, 2006.

(2) Scientific Personnel Supported

      1. Prof. Theodore B. Norris, Principal Investigator

      2. Hyunyong Choi, Graduate Student Research Assistant

Collaborators:

Laurent Diehl, Federico Capasso
School of Engineering and Applied Sciences, Cambridge, Massachusetts 02138, USA
Harvard University

Tobias Gresch, Marcella Giovannini, Jérôme Faist
Institute of Physics, University of Neuchâtel, CH-2000 , Neuchâtel, Switzerland

(3) Inventions

      No patents applied for.

(4) Scientific Progress and Accomplishments

      This research program accomplished several pioneering breakthroughs in the study and understanding of electronic dynamics in quantum cascade lasers (QCL's). Our initial work pioneered femtosecond time-resolved mid-infrared pump-probe experiments on quantum cascade lasers (QCL's). For the first reporting period, we carried out comprehensive time-resolved experiments on gain recovery dynamics in an operating QCL (samples based on 'diagonal transition' in real space provided by Prof. Capasso's group). Those data revealed that the speed of electron transport in cascade heterostructure is dramatically reduced due to the onset of quantum stimulated emission, as the oscillating intra-cavity laser field starts to derive the entire cascade structure, while applied static electric field plays a minor role.

      We subsequently showed that the gain recovery in QCL is qualitatively different from that in conventional atomic, molecular and interband semiconductor lasers: there is a strong coupling between each active region due to the superlattice transport component, enabling the transport physics to show a strong dependence of intra-cavity photon density. We developed a complete 3-level rate equation for the superdiagonal QCL level

population which is directly following from the computed bandstructure. This work was published in Phys. Rev. Lett. and Appl. Phys. Lett.

Following the pump-probe work, we then modified the setup to perform ultrafast upconversion of the QCl output following injection of a femtosecond pulse into a lasing QCl cavity. Our initial work focused on dispersive effects (published in Optics Express); our final work involved investigation of coherent effects in pulse propagation, and the direct observation for the first time in the time domain of Rabi oscillations on the gain transition of a semiconductor laser. Preliminary versions of that work were presented at various conferences; we have recently completed a theoretical model of the results which has put all the pieces together for a manuscript submitted to Nature Physics.

Background

Electronic transport is central to the understanding of the physics of solid state devices such as transistors, detectors, modulators, light emitting diodes and laser diodes [1]. The discovery of quantum phenomena in nanometer-thick layers, including size quantization [2, 3], the quantum confined Stark effect [4] and resonant tunneling [5] has greatly enriched semiconductor physics by enabling novel functionalities and devices. Here we investigate the transport of electrons through a quantum cascade laser (QCL) [6]; QCL's are particularly interesting as tools for investigating electronic transport, as they operate under conditions of fully developed quantum transport that cannot be described in the framework of drift-diffusion equations.

In a QCL, electrons cascade through the heterostructure, ideally emitting one photon via stimulated emission in each active region. Thus QCL operation results from a coupling of perpendicular drift transport with the intra-cavity optical field. In this Letter, we demonstrate remarkable changes in electronic transport across the device as the current is increased above threshold: from drift in the presence of phonon scattering to photon-driven transport via stimulated emission leading to a greatly reduced transit time across the entire length of the device. Our approach to studying the coupling of transport and laser dynamics is to time-resolve the dynamics of the gain recovery following an impulsive perturbation of the intra-cavity field. Pump-probe methods have previously been used to explore the possibility of coherent transport in resonant-tunnelling QC

6

structures [7] under non-lasing conditions [8]. Here, we explore the gain dynamics of operating QCL's below and above threshold, and the measured dynamics is used to develop a model for the QCL level populations coupled to the cavity photon density rate equation. We show that the transport is driven by the photon density, which is qualitatively different from previous photon-assisted tunneling studies [9, 10] in which an external classical field opens a new channel for transport.

QCL Sample Characteristics

Two QCL's were fabricated and processed with different cavity length and width: laser N-432 was 3.53 mm long and 12.5 μm wide, operating at 5.3 μm, and laser N-433 was 2.41 mm long and 17.1 μm wide, operating at 5.25 μm. The lasers used in this study (Fig. 1) are based on a 'diagonal transition' in real space [11]. A population inversion is present at all bias fields in these experiments; the cavity gain is controlled by voltage tuning of the oscillator strength through the linear Stark effect. The lowest state of the injector region serves as both the electron reservoir and also the upper lasing state. Laser action takes place between the upper state (level 2) and the lower state in the active region (level 1), which is emptied via tunneling into the superlattice. Before an electron can contribute to stimulated emission in the next active region (i.e. the portion of the cascade heterostructure in which the optical transition takes place), it must drift across the superlattice injector region.

Time-Resolved Experiments and Data Analysis

Gain recovery dynamics were investigated using ultrafast degenerate pump-probe techniques, with the QCL operating in continuous wave at a constant voltage. The pump and probe beams were coupled into the QCL waveguide (with polarizations ± 45° with respect to the lasing polarization, respectively), and the differential transmission (DT) of the weak probe pulse was measured following the saturation of the gain by a perturbing pump pulse; the pump and probe were tuned to be resonant with the gain transition at each bias. In Fig. 2(a), selected bias-dependent DT results at 30 K are displayed. For positive pump-probe delay, negative DT signals were observed at all bias currents. The

recovery of the DT can be understood as the gain recovery due to electron transport in the cascade heterostructure following the pump-induced gain depletion.

In a simple picture, one can see how the current is driven by the laser photon density in such a structure. In a cascade heterostructure, the current through a given level is given by $J=qN/\tau$, where q is the electron charge, N is the areal density, and τ is the state lifetime. Below threshold, the upper state lifetime is determined by (off-resonant) phonon-assisted tunneling (20-50 ps here). Above threshold, the relevant lifetime should become the stimulated emission lifetime τ_{st}.

The gain recovery was fit by solving the following three-level rate-equation model including coupling to a single mode cavity photon flux: an example of the fit at 0.635 A is shown in Fig. 2(b).

$$\frac{dS}{dt} = \left[N_P \Gamma_P v_g g_c (n_2 - n_1) - \frac{1}{\tau_p} \right] S + N_P \beta \frac{n_2}{\tau_{sp}}$$

$$\frac{dn_2}{dt} = \frac{n_{SL}}{\tau_{SL}} - \frac{n_2}{\tau_2} - \Gamma_P v_g g_c (n_2 - n_1) S$$

$$\frac{dn_1}{dt} = \frac{n_2}{\tau_2} - \frac{n_1}{\tau_1} + \Gamma_P v_g g_c (n_2 - n_1) S$$

$$\frac{dn_{SL}}{dt} = \frac{n_1}{\tau_1} - \frac{n_{SL}}{\tau_{SL}}$$

, where n_2, n_1, n_{SL} are the level-2, level-1, superlattice electron density, and S is the photon density. N_p is the number of stages in the QCL, Γ_p is the confinement factor for one period, v_g is the group velocity, g_c is the gain cross-section, τ_p is the photon lifetime, β is the spontaneous emission factor (fraction of spontaneous emission emitted into the lasing mode), τ_{sp} is the spontaneous emission lifetime, τ_{SL} is the superlattice transport time, τ_2 is the non-radiative lifetime of level 2, and τ_1 is the tunneling time from level 1 to the superlattice. We found that fits using fewer than three temporal components were unable to systematically fit the DT curves.

As can be seen in the rate equation, there are four processes that enter the dynamics: (i) phonon-assisted relaxation out of the upper lasing state, (ii) stimulated emission out of the upper lasing state, (iii) depletion of the lower lasing state via tunneling, and (iv) transport across the superlattice.

The central result is contained in Fig. 3, (a) and (b), which shows the upper state lifetime τ_2, obtained from the rate-equation fits of the DT data, as a function of bias current. Three processes contribute to the decay of the upper state: phonon-assisted intersubband relaxation [12] with time constant τ_{ph}, radiative decay by spontaneous emission τ_{rad}, and stimulated emission τ_{st}. The total upper state lifetime is given by $\tau_2^{-1}=\tau_{ph}^{-1}+\tau_{rad}^{-1}+\tau_{st}^{-1}$. Since τ_{rad} is several microseconds, radiative decay is negligible. Well below threshold, the upper state lifetime is essentially τ_{ph}, which is in the range of 20-50 ps. As the QCL bias voltage approaches threshold from below, stimulated transitions start to occur, reducing the upper state lifetime and increasing the current through the device. In Fig. 3, (a) and (b), a dramatic reduction in the upper state lifetime as the QCL approaches threshold is very clear for both devices. Above threshold, τ_{st} becomes of an order of a few ps, and does not appear in the DT gain recovery dynamics (i.e. above threshold the DT dynamics are determined entirely by the lower state emptying and the superlattice transport components).

This behavior is in strong contrast to that of conventional atomic or molecular lasers, or of semiconductor lasers based on interband transitions; for those lasers the gain recovery time constant is the spontaneous emission time τ_{sp} below threshold, and (in the short cavity-lifetime limit) τ_{ph} /r above threshold, where r is the ratio of the pump rate to the threshold pump rate [13]. The QCL gain recovery curves in Fig. 2 and 3 show, however, an order-of-magnitude speed-up in the gain recovery at threshold. The differences in gain recovery between QCL's and atomic, molecular, and interband semiconductor lasers can be traced to a combination of several unique features of QCL's.

The most important difference is that the gain recovery in QCL's has a component that has no analogue in conventional laser systems, namely the transport delay between active regions in the cascade structure. If this mechanism is removed from the rate equations, then those equations become the same as in conventional lasers, and the order-of-magnitude speed-up of the gain recovery just below threshold due to stimulated emission is not seen. Each active region in a QCL is essentially an open system, coupled by transport through the superlattice to adjacent active regions; once an electron has made a downward transition via stimulated emission, it is not re-pumped into the excited state within the same active region. Instead it must be transported to the next

active region, with a corresponding delay. By contrast, stimulated emission in conventional lasers occurs in a closed system; following a downward transition, an electron is re-pumped into the excited state within the same atom or molecule.

The second contributing factor to the dramatic speed-up in gain recovery near threshold is the interplay of the non-radiative nature of the upper state decay far below threshold, and the turn-on of stimulated emission just below threshold. Well below threshold, the phonon-assisted lifetime is weakly bias-dependent. Just below threshold, the photon density in the cavity becomes of the order of a few hundred, which is sufficient to drive the stimulated emission lifetime down to a value comparable to the non-radiative lifetime. (It is also an important feature of QCL's that the β factor is rather high, approximately 10^{-3}, as obtained from the L-I curves). Above threshold, the stimulated lifetime continues to decrease as the current increases, but it no longer appears in the gain recovery dynamics (as the gain recovery is limited in that case only by the lower state tunnelling and superlattice transport delays).

The self-consistency of the model used to understand the gain recovery dynamics was verified by the following procedure. First, we calculated τ_{st} via the three-level rate-equation model (blue solid line in Fig. 3, (a) and (b)), and found good agreement with the DT data. Secondly, we also calculate τ_{st} via an estimate of the intra-cavity photon density obtained from the measured steady-state L-I characteristic; this appears as the black and green solid line in the Fig. 3, a and b, respectively. Finally, to check self-consistency, the rate equations used to fit the dynamics were solved in steady-state to obtain the threshold current and steady-state L-I curves; these are seen in Fig. 3(c) to agree quite well with the experiment.

In addition to the upper state lifetime, two other components are obtained in fits to the gain recovery dynamics (Fig. 4) [14]. The fastest component τ_1, approximately 0.7 ps, corresponds to the decay of the lower lasing state via tunneling. The second component, on the time scale of 2 ps, shows a characteristic inverse dependence on the bias current. We have observed this component in a variety of different QCL structures, and attribute it to the superlattice transport. We note that contributions from carrier heating and waveguide anisotropy were experimentally shown to be small ($\leq$0.1 %) [14].

Ultrafast Coherent Pulse Propagation

In the coherent light-matter interaction regime, a pulse propagating through an absorber with area on the order of pi leads to coherent oscillations of the population (Rabi oscillation), leading to the McCall-Hahn area theorem [15]. Rabi flopping in a semiconductor is usually hindered due to a rapid dephasing process that may occur on a time scale as fast as several tens of femtoseconds at elevated carrier density and temperature, compared to an order of 2 or 3 lower rates in an atomic system [16]. On the other hand, semiconductor intersubband transitions afford the possibility of obtaining very large dipole transition matrix elements, leading to the possibility of Rabi flopping at the small pulse energies present in quantum cascade lasers. Indeed, coherent effects in semiconductor lasers were first seen as sidebands in the spectra of a QCL arising from a modulation of the gain at the Rabi frequency Ω_R [17]. In this work we investigate pulse propagation in the time domain, and directly observe the Rabi oscillation in the QCL gain.

Our approach is to investigate the time-evolution of transient laser output followed by ultrashort resonant pulse injection into an operating QCL [18]. The low temperature (30 K) L-I characteristics of our QCL [19] are shown in Fig. a. The QCL spectra show significant spectral broadening above threshold, stemming from spatial-hole burning and multi-mode instabilities, the latter due to the enhanced dipole matrix element [17]. As discussed later, the dynamic interaction between the QCL and the ultrashort pulse is modelled by three-level Maxwell-Bloch equations (Fig. b). The three-level model describes the essential physics of the QCL that includes the populated lasing state (level 3), the depopulated lasing state (level 2) and the extracted ground state (level 1). A schematic of our experiment is displayed in Fig. c, where we employ an ultrafast time-resolved cross-correlation technique to measure the intensity dynamics of the QCL output. Figure d shows a typical cross-correlation measurement signal after resonant mid-infrared (IR) pulse injection (FWHM, 150 fs) gated by 800 nm pulse (FWHM, 120 fs). The center wavelength of the mid-IR pulse (~ 5 µm) is tuned to be resonant with the QCL emission wavelength. The bandwidth of the mid-IR spectrum almost covers the electroluminescence spectrum of the QC structure as well as the entire QCL spectrum operating above threshold (not shown). All measurements are performed with a QCL bias of 1.5 times above threshold and at a cold finger temperature of 30 K.

Our key experimental observations are shown in Fig. 5 (e-h). We monitor both the propagated mid-IR pulse through the QCL and the transient changes of the lasing dynamics for three different pulse areas Θ. For the envelopes of the propagated pulses (Fig. e), noticeable features are the dramatic advance of the peak envelope to earlier times and significant reshaping as Θ increases. For example, there is a negligible time shift and envelope distortion when Θ is π. When Θ increases to 2π, the time advance of the envelope peak is about 38 fs, and this time shift reaches to as much as 81 fs for Θ approaching 3π with substantial envelope reshaping (blue arrow in Fig. e). For the lasing dynamics (Fig. g), the magnitude of the laser output transient decreases after the pulse by as much as 59 % (compared to the lasing intensity before the pulse) when Θ is π (black curve), and it further decreases to about 64 % when Θ reaches 2π (red curve). However, when Θ approaches 3π, the transient dynamics is weakly visible, showing no significant saturation of the lasing intensity (blue curve).

The central observation is the contribution of the coherent dynamics between the propagating resonant optical pulse and the density-dipole oscillation in the QCL. The numerical simulations of the three-level Maxwell-Bloch equations are shown in Fig. 5 (f and h), and directly compared to the experiments. The envelope reshaping of the propagated pulse (Fig. 5f) and the lasing dynamics (Fig. 5h) agree well with the experiments (Fig. 5e and5 g). Simulated density and dipole polarization (not shown) reveal that the Rabi oscillation frequency Ω_R becomes larger than the dephasing rate as increasing Θ. In this regime, the dipole polarization is coherently cycled due to Rabi flopping, and resulting in the time advance and reshaping of the pulse envelope and the reduction in the circulating laser intensity due to coherent reduction in the gain following the injected pulse. These results are potentially important for possible new pulse-generation methods in QCL's [20].

Conclusion

In conclusion, time-resolved measurements of the gain recovery dynamics in cascade heterostructure lasers show that the transport through the device and the cavity photon density are intimately coupled, and that from just below to above threshold, the current through the device is determined by the stimulated emission rate into the lasing

12

mode. We note that analogous tunnelling of electrons via a photon-assisted transition has been previously observed in resonant tunnelling devices under the application of an external oscillating electric field [9, 10]. In those experiments, the presence of a strong external classical field opened up a new channel, increasing the transport across the device. In QCL's the current near and above threshold is driven by the intra-cavity photon density, and the effect of quantum stimulated emission on transport at the few-photon level can be seen to turn on as the laser approaches threshold from below.

When short pulses are injected into the lasing cavity, and the pulse area is sufficiently large (pi-pulse), then coherent effects may be observed on the lasing transition, and specifically Rabi oscillation of the population inversion may be observed.

References

[1] S. M. Sze., *Physics of Semiconductor Devices*, (John Wiley & Sons, New York, 1981).

[2] Dingle, R., W. Wiegmann and C. H. Henry, Phys. Rev. Lett. **33**, 827 (1974).

[3] L. L. Chang, L. Esaki, and R. Tsu, Appl. Phys. Lett. **24**, 593 (1974).

[4] D. A. B. Miller *et al.*, Phys. Rev. Lett. **53**, 2173 (1984).

[5] T. C. L. G. Sollner *et al.*, Appl. Phys. Lett. **43**, 588 (1983).

[6] J. Faist *et al.*, Science **264**, 553 (1994).

[7] F. Eickemeyer *et al.*, Phys. Rev. Lett. **89**, 47402 (2002).

[8] R. C. Iotti and F. Rossi, Phys. Rev. Lett. **87**, 146603-1 (2002); S. C. Lee *et al.*, Phys. Rev. B **73**, 245320-1 (2006); C. Weber *et al.*, Appl. Phys. Lett. **89**, 091112-1 (2006).

[9] A. H. Dayem and R. J. Martin, Phys. Rev. Lett. **8**, 246 (1962); P. K. Tien and J. P. Gordon, Phys. Rev. **129**, 647 (1963).

[10] P. S. S. Guimaraes *et al.*, Phys. Rev. Lett. **70**, 3792 (1993); B. J. Keay *et al.*, Phys. Rev. Lett. **75**, 4098 (1995); B. J. Keay *et al.*, Phys. Rev. Lett. **75**, 4102 (1995); K. Unterrainer *et al.*, Phys. Rev. Lett. **76**, 2973 (1996).

[11] J. Faist *et al.*, Nature **264**, 387 (1997).

[12] D. Y. Oberli *et al.*, Phys. Rev. B **40**, 3028 (1989).

[13] A. E. Siegman, *Lasers*, (University Science Books, Sausalito, California, 1986).

[14] Hyunyong Choi, Laurent Diehl, Tobias Gresch, Marcella Giovannini, Jérôme Fais, and Federico Capasso, Theodore B. Norris, "Femtosecond Dynamics of Resonant

Tunneling and Superlattice Transport in Quantum Cascade Lasers," to be submitted to Appl. Phys. Lett., 2007; Hyunyong Choi, Zong-Kwei Wu, Theodore B. Norris, Tobias Gresch, Marcella Giovannini, Jérôme Fais, Laurent Diehl and Federico Capasso, "Time-Resolved Investigation of Ultrafast Carrier Dynamics in Quantum Cascade Lasers", to be submitted to IEEE J. Quantum Electron., 2007.

[15] L. Allen and J. H. Eberly, Optical resonance and two-level atom (Dover, New York, 1987); S. L. MaCall and E. L. Hahn, Phys. Rev. Lett. 18, 908 (1967).

[16] A. E. Siegman, Lasers (University Science Books, Sausalito, California, 1986).

[17] C. Y. Wang, et al., Phys. Rev. A 75, 031802 (2007); A. Gordon, et al., Phys. Rev. A 77, 053804 (2008).

[18] H. Choi, et al., Opt. Express, 15, 15898 (2007); H. Choi, et al., in Proceedings of the Conference on Lasers and Electro-Optics, San Jose, (2008).

[19] L. Diehl, et al., Appl. Phys. Lett. 88, 2011151 (2006).

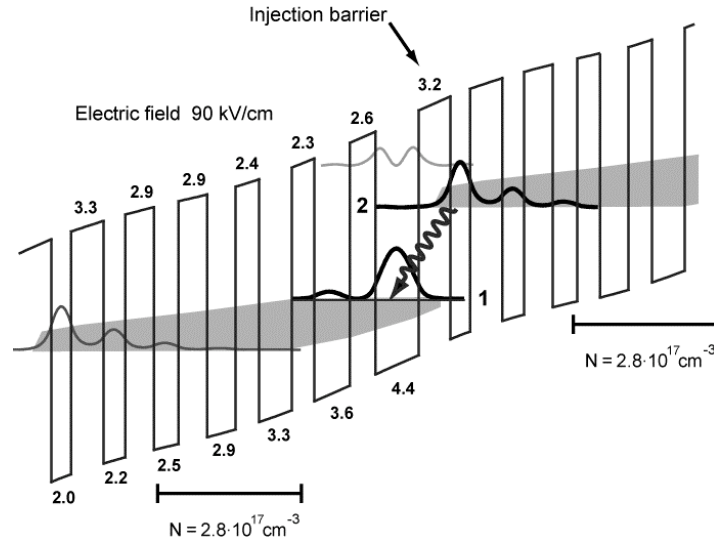[20] C. R. Menyuk and M. A. Talukder, Phys. Rev. Lett. 102, 023903 (2009).

Figures

Injection barrier

Electric field 90 kV/cm

$N = 2.8 \cdot 10^{17} cm^{-3}$

$N = 2.8 \cdot 10^{17} cm^{-3}$

Figure 1 Schematic conduction band diagram and measured L-I-V curve for QCL from N-432. Self-consistent band structure calculation of the $In_{0.6}Ga_{0.4}As/In_{0.44}Al_{0.56}As$ strained layer sequence for two periods of the cascade heterostructure, at a bias corresponding to an internal electric field of 90 kV/cm, is displayed. Layer thicknesses are given in nm. The wavefunctions for the upper (level-2) and lower lasing state (level-1) are shown, illustrating the diagonal nature of the transition in real space. The wavy arrow indicates the lasing transition. The miniband is indicated by the shaded gray region. The horizontal segments show the doped region for each period; N is the donor density.
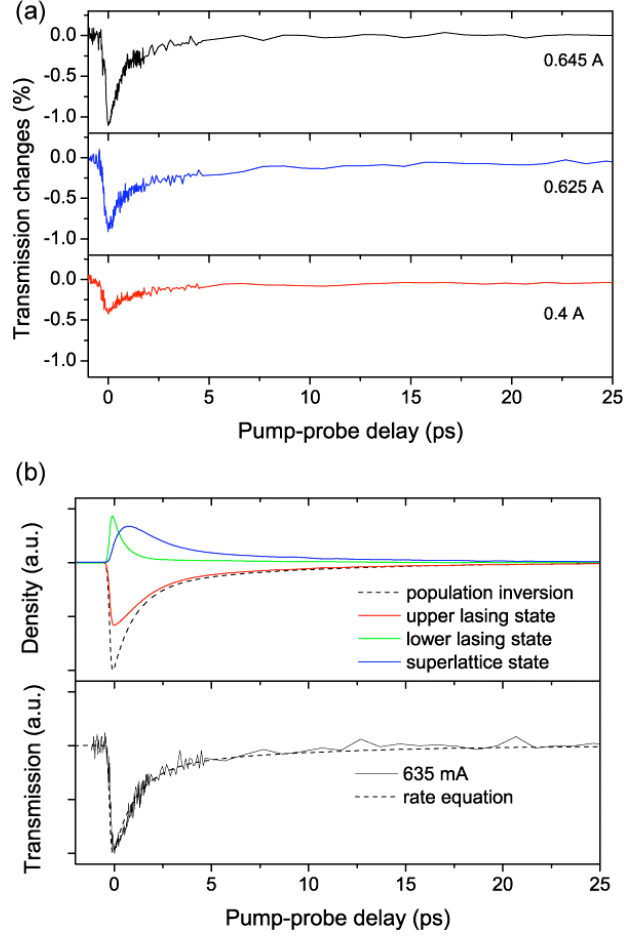
Figure 2 Bias-dependent DT measurements of the gain recovery at 30 K for QCL from N-432. (b) 3-level rate-equation simulation on the population dynamics of upper state, lower state and superlattice state (upper panel) and a fit to the the normalized DT signal at 0.635 A (lower panel) are displayed.
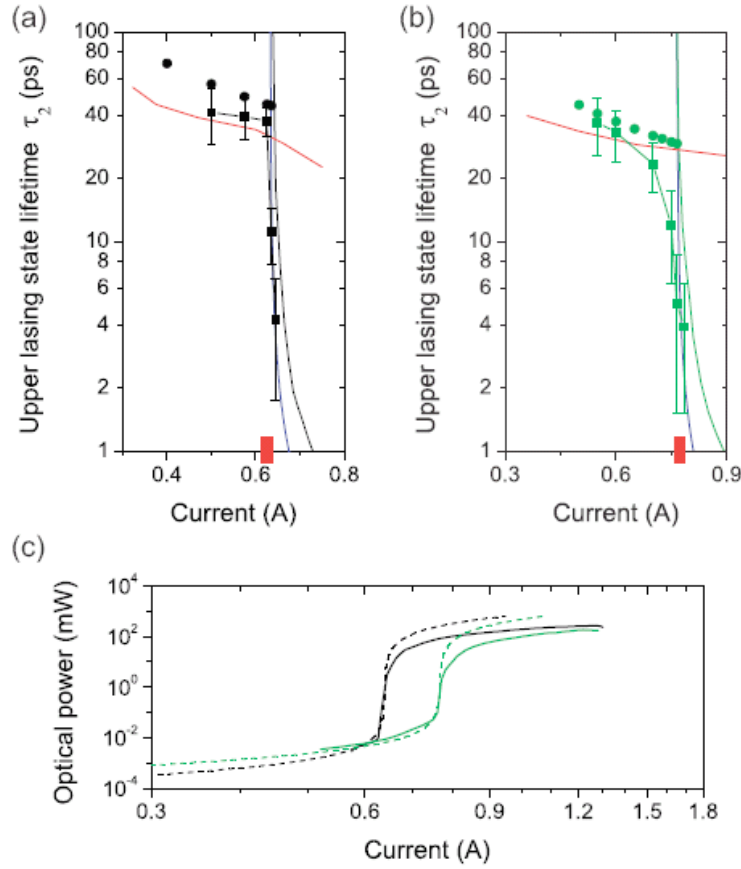
Figure 3 Bias-dependent level-2 lifetime τ_2 is shown for N-432 in (a) and N-433 in (b) (threshold is indicated by the red tick mark). The filled squares are the level-2 lifetime obtained from rate-equation fits to the gain recovery DT data. The red solid lines in (a) and (b) are the level-2 lifetime due to optical-phonon scattering calculated using the bias-dependent wavefunctions; the errors obtained by assuming monolayer fluctuations of the barrier width are around 10 ps, which is within our measurement. The filled circles are an estimate of the level-2 lifetime using $J=qN/\tau_2$ and assuming the level-2 population N is simply the doping density. The dramatic reduction in lifetime just below threshold corresponds to the onset of stimulated emission. The stimulated emission lifetime

τ_{st} was obtained in two ways, using the L-I curves shown in (c). First, τ_{st} was calculated directly by obtaining the cavity photon density S from the measured output power (solid line in (c)) and using $\tau_{st} = N/v_g N_p g_c S$, where N is the population inversion (again assumed to be the doping density), v_g is the group velocity, N_p is the number of cascading stages (=25 in our QCL), and g_c is the gain cross-section; the result is shown as the black and green solid vertical line in (a) and (b), respectively. Secondly, the rate-equation model was used to fit the L-I curves (dashed line in (c)), and the resulting values of S were used to calculate v_{st}. The result is the blue solid vertical line in (a) and (b). The only free parameter required to fit the L-I curves with the rate-equation model is the β factor.
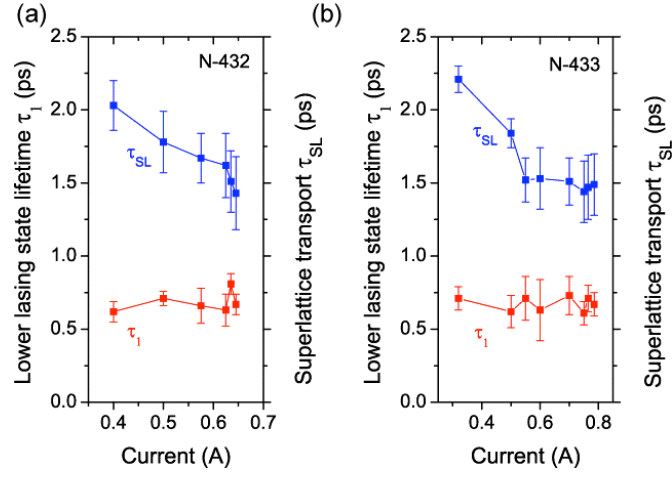
Figure 4 (a)**,** Extracted time constants for N-432 from the rate-equation fit. τ_1 is the level-1 lifetime (red), and τ_{SL} is the time constant of gain recovery due to the superlattice transport (blue), as explained in the text. (b)**,** Extracted time constants for N-433 from the 3-level rate-equation fit. τ_1 and τ_{SL} have same meaning as in (a). The error bars are determined from the chi-square values obtained in the rate-equation fit.
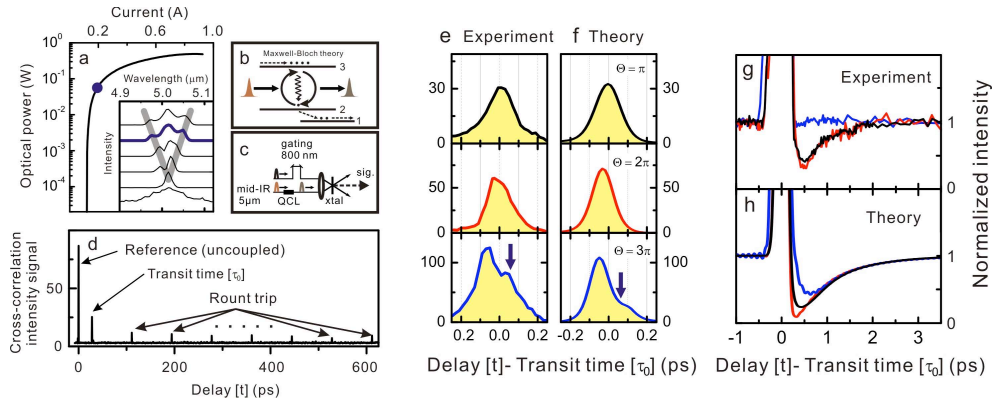
Fig. 5. (a) Low-temperature light vs. current (L-I) characteristics (30 K) of a QCL used in this study. The QCL emission spectra are shown in the inset, starting with below threshold and above threshold spectrum. Thick blue curve is the spectrum taken for this measurement (1.51 times above threshold, marked as a blue dot in the L-I curve). (b) QCL is modelled using three-level Maxwell-Bloch equations for theoretical analysis. (c) A schematic setup of the ultrafast time-resolved cross-correlation measurement using 250-kHz regenerative amplifier laser system (Coherent RegA). (d) A typical cross-correlation signal is displayed when the QCL biased near threshold. The uncoupled mid-IR pulse is used as a reference time-zero delay. Once the pulse is coupled, the propagating pulse experiences a transit time delay and several round-trip delays. (e) Experimentally measured propagated pulse envelopes and (f) Maxwell-Bloch simulations are displayed. For direct comparison, all curves are plotted on a single time axis; the transit time $[\tau_0]$ is subtracted from the gating delay time $[t]$, using a reference time line as the π pulse interaction case. The measured (g) and calculated (h) transient lasing dynamics are shown at different pulse area (black, red and blue curves are for a π, 2π, and 3π pulse, respectively).